Research Square

Preprints are preliminary reports that have not undergone peer review.
They should not be considered conclusive, used to inform clinical practice,
or referenced by the media as validated information.

ω-3 PUFAs Attenuate Postoperative Ileus by Modulating the NLRP3/Caspase-1/IL-1β Inflammatory Axis

Liuchuang Zhang
Affiliated Hospital of Nanjing University of Chinese Medicine
haoran Gu
Affiliated Hospital of Nanjing University of Chinese Medicine
jing Yu
Affiliated Hospital of Nanjing University of Chinese Medicine
xuan Zhao
Affiliated Hospital of Nanjing University of Chinese Medicine
yiting Li
Affiliated Hospital of Nanjing University of Chinese Medicine
huafeng Pan
Jiangsu Province Hospital of Chinese Medicine, Affiliated Hospital of Nanjing University of Chinese Medicine
haifeng Wang
Jiangsu Province Hospital of Chinese Medicine, Affiliated Hospital of Nanjing University of Chinese Medicine
miaomiao Ge
Jiangsu Province Hospital of Chinese Medicine, Affiliated Hospital of Nanjing University of Chinese Medicine
zhiwei Jiang
surgery340163.com

Jiangsu Province Hospital of Chinese Medicine, Affiliated Hospital of Nanjing University of Chinese Medicine
Gang Wang
Affiliated Hospital of Nanjing University of Chinese Medicine

Article

Keywords: ω-3 PUFAs, postoperative ileus, macrophage polarization, NLRP3/Caspase-1/IL-1β inflammatory axis, pyroptosis

Posted Date: November 3rd, 2026

DOI: https://doi.org/10.21203/rs.3.rs-10965722/v1

License: This work is licensed under a Creative Commons Attribution 4.0 International License.
Read Full License

Additional Declarations: No competing interests reported.

Abstract

Postoperative ileus (POI) is partly driven by intestinal inflammation and macrophage activation. We investigated whether omega-3 polyunsaturated fatty acids (ω-3 PUFAs) alleviate POI by modulating macrophage polarization and NLRP3 inflammasome signaling. C57BL/6 mice with intestinal manipulation-induced POI received different doses of ω-3 PUFAs. Ileal injury, intestinal transit, inflammatory mediators, macrophage phenotypes, and inflammasome-related proteins were assessed, and data-independent acquisition proteomics was used to identify candidate pathways. In vitro, PMA-differentiated THP-1 macrophages were stimulated with lipopolysaccharide and ATP, with MCC950 used as an NLRP3 inhibitor control. ω-3 PUFAs reduced ileal injury, preserved villus architecture, improved intestinal transit and smooth muscle-related markers, and decreased IL-1β and IL-18 levels in POI mice. Proteomics highlighted the NOD-like receptor signaling pathway. ω-3 PUFAs also reduced macrophage infiltration and M1-like polarization, promoted M2-like polarization, and suppressed NLRP3 inflammasome activation, Caspase-1 activation, and GSDMD-mediated pyroptosis in vivo and in vitro. These findings indicate that ω-3 PUFAs alleviate POI-associated intestinal inflammation and dysmotility by modulating macrophage polarization and suppressing NLRP3/Caspase-1/IL-1β signaling, supporting their potential as a nutritional intervention for POI.

Introduction

POI is a frequent gastrointestinal motility dysfunction that occurs after abdominal surgery. Clinically, it is manifested by abdominal pain, abdominal distension, nausea, vomiting, poor tolerance of oral intake, and delayed passage of flatus or stool, all of which can hinder postoperative recovery and negatively affect patients' quality of life [1, 2]. Although enhanced recovery after surgery (ERAS) strategies have made substantial advances in decreasing postoperative complications and improving clinical outcomes, the management of POI is still mainly supportive. At present, several adjunctive interventions, including gum chewing, electroacupuncture, and prokinetic drugs, are commonly used to facilitate the restoration of intestinal motility [3]. Nevertheless, epidemiological data from the United States indicate that the incidence of POI among patients undergoing abdominal surgery is approximately 10%–30%, with associated annual healthcare costs reaching up to 1.47 billion US dollars [4–5]. Therefore, identifying safe and effective therapeutic strategies to prevent or alleviate POI has important clinical implications for promoting postoperative recovery and easing the healthcare burden.

The pathogenesis of POI is complex, among which inflammatory responses are considered to play a central role[6–8]. During surgery, intestinal manipulation, including traction, compression, and exposure of the bowel, induces local tissue injury and the release of damage-associated molecular patterns (DAMPs), thereby activating resident macrophages within the intestinal muscularis. Activated macrophages contribute to inflammatory signaling through two major mechanisms. On the one hand, DAMPs activate the TLR signaling pathway, leading to the upregulation of NLRP3, pro-IL-1β, and other inflammation-related molecules. On the other hand, NLRP3 inflammasome assembly can be further driven by ATP release, K^+ efflux, excessive reactive oxygen species (ROS) production, and mitochondrial

dysfunction Subsequently, the NLRP3 inflammasome recruits ASC and activates Caspase-1, thereby promoting the processing and secretion of inflammatory mediators, including IL-1β and IL-18, which further induce inflammatory cell infiltration and amplify the inflammatory cascade[9–13]. Persistent inflammation within the intestinal muscularis can inhibit enteric neurotransmitter release, impair the rhythmic activity of interstitial cells of Cajal, and reduce smooth muscle contractility through nitric oxide, prostaglandins, and pro-inflammatory cytokines, ultimately resulting in delayed gastrointestinal transit [14–18].

ω-3 PUFAs, primarily including eicosapentaenoic acid (EPA) and docosahexaenoic acid (DHA), are bioactive fatty acids with essential physiological roles. Accumulating evidence indicates that ω-3 PUFAs mediate inflammation-suppressive effects through diverse mechanisms. Their bioactive metabolites can interact with membrane-bound or nuclear receptors, inhibit Toll-like receptor signaling, and suppress transcription factors including NF-κB, consequently reducing the secretion of inflammatory mediators such as TNF-α, IL-1β, and IL-18 [19, 20]. Previous studies have demonstrated that transgenic mice with enhanced endogenous conversion of n-6 PUFAs to n-3 PUFAs exhibited increased tissue ω-3 PUFA levels, which promoted anti-inflammatory protein production and alleviated colitis and tissue damage. These beneficial effects may be partly attributed to reduced NF-κB activation and decreased expression of TNF-α, inducible nitric oxide synthase, and IL-1β [21].

However, studies investigating the effects and mechanisms of ω-3 PUFAs in POI remain limited. In particular, systematic investigations linking intestinal muscularis macrophages, inflammasome-mediated inflammatory signaling, and restoration of intestinal function are still lacking. Based on this rationale, the present study established both in vivo and in vitro models and employed hematoxylin and eosin staining, immunofluorescence, immunohistochemistry, Western blotting, ELISA, and proteomic analysis to systematically investigate whether ω-3 PUFAs regulate POI through the NLRP3/Caspase-1/IL-1β inflammatory pathway. The findings are expected to provide new mechanistic evidence and intervention clues for clinically preventing and treating POI.

Materials and Methods

Reagents

The ω-3 PUFA preparation used in this study was purchased from Nanjing Shishi Biotechnology Co., Ltd. (Nanjing, China). Eicosapentaenoic acid (EPA, #E44864) and docosahexaenoic acid (DHA, #D2534) were purchased from Sigma-Aldrich (St. Louis, MO, USA). Primary antibodies against NLRP3 (#15101), Caspase-1 (#24232), ASC (#67824), GSDMD (#39754), IL-1β(#12242) and Caspase-1 p20 (#89332) were obtained from Cell Signaling Technology (Danvers, MA, USA). β-actin antibody (ZB15001-HRP-100) was obtained from Servicebio Technology Co., Ltd. (Wuhan, China). Goat anti-mouse secondary antibody (RGAM001) and goat anti-rabbit secondary antibody (RGAR001) were obtained from Proteintech Group, Inc. (Wuhan, China). ELISA kits for detecting IL-1β and IL-18 were supplied by Epizyme Biomedical

Technology Co., Ltd. (Shanghai, China), whereas the IL-10 ELISA kit was purchased from Elabscience Biotechnology Co., Ltd. (Wuhan, China).

Animals and POI Model

A total of 50 male C57BL/6 mice, aged 6–8 weeks and weighing 20–22 g, were provided by Beijing Vital River Laboratory Animal Technology Co., Ltd. All mice were housed under specific pathogen-free (SPF) conditions with controlled temperature and humidity, maintained on a 12 h light/dark cycle, and allowed free access to food and water. C57BL/6 mice were fasted for 12 h before surgery. Preoperative preparation included administration of tribromoethanol anesthesia, sterilization of surgical instruments, and maintenance of body temperature at 37.5°C using a heating pad. The anesthetic was administered intraperitoneally at a dose of 0.2 mL/10 g body weight to ensure complete anesthesia for approximately 20 min.After anesthesia, the abdominal hair was removed and the midline abdominal area was disinfected. The small intestine was gently exteriorized using saline-moistened cotton swabs, and uniform pressure was applied along the small intestine from the proximal to the distal segment for 5 min until small hemorrhagic spots appeared on the intestinal surface, thereby mimicking intraoperative mechanical injury. The small intestine was then returned to the abdominal cavity, followed by administration of 100 μL sterile saline for fluid replacement. The muscular layer and skin were sutured separately, and the mice were placed in a 37.5°C heated environment until recovery from anesthesia [22].

Fifty mice were randomly allocated into five groups: Sham, POI, ω3-L, ω3-M, and ω3-H, with 10 mice per group. After surgery, animals in the Sham and POI groups were administered 0.2 mL saline by oral gavage twice daily. In contrast, mice in the ω3-L, ω3-M, and ω3-H groups were treated with ω-3 PUFA fish oil emulsion at doses of 0.14, 0.21, and 0.28 g/kg, respectively. The treatment was administered by gavage at 100 μL/10 g body weight twice daily for two consecutive days. At 12 h after the last administration, the mice were sacrificed by cervical dislocation. At the experimental endpoint, mice were deeply anesthetized with isoflurane. After the absence of the pedal withdrawal reflex was confirmed, the mice were euthanized by cervical dislocation. Death was confirmed by the cessation of respiration and heartbeat before tissue collection. Ileal tissues were then harvested, gently flushed to remove intestinal contents, rapidly frozen in liquid nitrogen and preserved at − 80°C for later experiments. All animal procedures were reviewed and approved by the Ethics Committee of the Affiliated Hospital of Nanjing University of Chinese Medicine (Approval No. 2026DW-084-01).

Cell Culture and Treatment

The human monocytic leukemia cell line THP-1 was supplied by Procell (Wuhan, China). Cells were cultured in RPMI-1640 supplemented with 10% fetal bovine serum and 1% penicillin–streptomycin under standard culture conditions at 37°C with 5% CO_2 in a humidified incubator. Cells at the logarithmic growth stage were selected for the following experiments.

DHA and EPA were dissolved in anhydrous dimethyl sulfoxide (DMSO) to prepare 100 mM stock solutions, which were stored at − 80°C protected from light. Before use, the stock solutions were diluted to the indicated working concentrations, and The final DMSO concentration was kept below 0.1%. THP-1 cells were initially treated with phorbol 12-myristate 13-acetate (PMA) to induce differentiation into macrophage-like cells, with subsequent DHA and EPA pretreatment and subsequent stimulation with LPS/ATP. An inflammasome activation model was established using lipopolysaccharide (LPS) combined with adenosine triphosphate (ATP) [17–19, 23].

According to the experimental design, cells were divided into six groups: blank control group (untreated), DHA and EPA alone-treated group (50 μM, 24 h), model group (LPS at 500 ng/mL for 3 h followed by ATP at 5 mM for 1 h), DHA + EPA low-dose group (pretreatment with 25 μM DHA + EPA for 24 h prior to LPS/ATP stimulation), DHA + EPA high-dose group (preincubated with 50 μM DHA/EPA for 24 h prior to LPS/ATP stimulation), and inhibitor group (pretreatment with MCC950 at 10 μM for 1 h followed by LPS/ATP stimulation) [24]. In this model, LPS served as the first signal for inflammasome activation by upregulating the expression of NLRP3 and pro-IL-1β, whereas ATP acted as the second signal to promote inflammasome assembly and Caspase-1 activation, thereby establishing a classical in vitro NLRP3 inflammasome activation model.

The effect of ω-3 PUFAs on THP-1 cell viability was determined using a CCK-8 assay. Briefly, THP-1 cells were plated in 96-well plates at 1 × 10^5 cells per well and allowed to stabilize. The cells were then exposed to different concentrations of DHA/EPA for 24 h, followed by incubation with CCK-8 reagent for 2 h. Absorbance was recorded at 450 nm, and cell viability was calculated to determine concentrations without evident cytotoxicity.

DIA-Based Quantitative Proteomic Analysis

To identify the potential molecular mechanisms by which ω-3 PUFAs ameliorate postoperative ileus, ileal tissues from mice in the Sham, POI, and ω-3 PUFA-treated groups were subjected to data-independent acquisition (DIA)-based quantitative proteomic analysis. Tissue samples were removed from − 80°C storage and kept on ice. Samples were finely pulverized under liquid nitrogen-precooled conditions, and total proteins were extracted with lysis buffer supplemented with 8 M urea and 1% protease inhibitor. Following ultrasonic disruption, the lysates were subjected to centrifugation at 15,000 × g for 10 min at 4°C. The clarified supernatants were harvested, and protein concentrations were measured using a bicinchoninic acid (BCA) protein assay.

Equivalent quantities of protein from each sample were processed by dithiothreitol (DTT)-mediated reduction and iodoacetamide (IAA)-mediated alkylation prior to trypsin digestion. Protein digestion was then carried out with trypsin using the filter-aided sample preparation method. The resulting peptides were acidified, purified with Strata X cartridges, lyophilized under vacuum, and then reconstituted. Peptide levels were determined using the Pierce™ Quantitative Peptide Assays & Standards kit.

Peptide mixtures were separated on a Vanquish Neo nano-flow liquid chromatography platform and subjected to DIA-based analysis using an Astral high-resolution mass spectrometer. Data acquisition was conducted in positive ion mode. The MS1 spectra were collected over an m/z range of 380–980, while MS2 data were obtained in DIA mode with 299 scanning windows. The isolation width was 2 m/z, and higher-energy collisional dissociation (HCD) was performed at a collision energy of 25 eV.

Raw MS data were analyzed with DIA-NN software for protein identification and quantitative analysis. Trypsin was selected as the digestion enzyme, with a maximum of one missed cleavage allowed. Cysteine carbamidomethylation was defined as a fixed modification, whereas methionine oxidation and protein N-terminal acetylation were selected as variable modifications. The false discovery rate (FDR) was maintained at < 1% at both peptide and protein levels.

Following normalization, the protein quantification data were used for subsequent bioinformatic analyses, including principal component analysis, sample correlation assessment, identification of differentially expressed proteins, and functional enrichment analysis. Differentially expressed proteins were defined based on a P value < 0.05 and a fold change > 1.3 or < 0.77. Gene Ontology (GO) annotation, Kyoto Encyclopedia of Genes and Genomes (KEGG) pathway analysis, and gene set enrichment analysis (GSEA) were further conducted. Given its relevance to inflammasome activation and pyroptosis, the NOD-like receptor signaling pathway was specifically examined. Moreover, pyroptosis- and NLRP3 inflammasome-related molecules, including NLRP3, ASC/Pycard, Caspase-1, IL-1β, and IL-18, and GSDMD, were selected for heatmap visualization and further experimental validation.

Immunohistochemistry

Ileal tissues were fixed with 4% paraformaldehyde for 24 h, routinely paraffin-embedded, and sectioned at 4 μm. The slides were then dewaxed using xylene, rehydrated using a graded ethanol series, and then processed for antigen retrieval. After nonspecific binding was blocked, the sections were incubated with primary antibodies overnight at 4°C and then treated with horseradish peroxidase (HRP)-conjugated secondary antibodies for 45 min at room temperature. Immunoreactive signals were visualized with 3,3'-diaminobenzidine (DAB), and nuclei were counterstained with hematoxylin. After dehydration, clearing, and mounting, the sections were examined under a light microscope Brown DAB staining was considered positive for target protein expression, while nuclei appeared blue. For each group, at least five randomly chosen fields were captured, and positive staining was semi-quantified using ImageScope software. All assays were conducted in at least three independent experiments.

Immunofluorescence Staining

Ileal samples were fixed with 4% paraformaldehyde, routinely embedded in paraffin, and sectioned at 4 μm. After dewaxing in xylene and rehydration through graded ethanol, the sections underwent antigen retrieval. Once cooled to room temperature, the slides were rinsed with PBS and blocked with 5% BSA or normal goat serum for 1 h to reduce nonspecific binding.

To evaluate macrophage accumulation and polarization in ileal tissues, the tissue sections were incubated with primary antibodies against F4/80, CD86, and CD206. After washing with PBS, the sections were incubated with appropriate fluorophore-labeled secondary antibodies for 1 h at room temperature protected from light. Cell nuclei were stained with DAPI, and the slides were coverslipped using antifade mounting medium. Fluorescence images were captured with a fluorescence microscope or laser scanning confocal microscope.

F4/80 was used as a macrophage marker, CD86 served as a marker for M1-like pro-inflammatory macrophages, whereas CD206 marked M2-like macrophages with anti-inflammatory and reparative properties. At least five randomly selected non-overlapping fields from each group were analyzed. Images were acquired using an Olympus BX53 fluorescence microscope and captured using the Pannoramic SCAN II system.

For cellular immunofluorescence colocalization analysis, THP-1 cells were seeded onto coverslips and subjected to DHA/EPA pretreatment and LPS/ATP stimulation according to the experimental grouping. After treatment, the cells were washed with PBS, fixed with 4% paraformaldehyde for 20 min, permeabilized with 0.1% Triton X-100 for 15 min at room temperature, and blocked with 5% BSA for 1 h. The cells were then incubated with primary antibodies against NLRP3 and ASC overnight at 4°C in the dark. After washing, the cells were incubated with the corresponding fluorophore-conjugated secondary antibodies for 1 h at room temperature in the dark, followed by nuclear counterstaining with DAPI and mounting. Images were acquired using a fluorescence microscope or a laser scanning confocal microscope. Colocalization of NLRP3 and ASC was used to evaluate inflammasome assembly. Fluorescence images were analyzed using ImageJ software, and the degree of colocalization between NLRP3 and ASC was assessed using Pearson's correlation coefficient or Manders' overlap coefficient. All image acquisition and quantitative analyses were performed under identical exposure settings and conducted in a blinded manner.

Histological Analysis

After fixation in 4% paraformaldehyde for 24 h, ileal tissues underwent routine histological processing, including dehydration, paraffin infiltration, and embedding. The prepared tissue sections were subjected to hematoxylin and eosin (HE) staining, followed by observation under a light microscope. HE-stained images were analyzed quantitatively using ImageJ software. For each mouse, at least five randomly selected non-overlapping fields were evaluated. Villi and crypts with complete morphology and uniform orientation were selected for measurement in each field. Villus height was measured from the villus apex to the crypt opening, while crypt depth was measured from the crypt opening to the crypt base. The villus height-to-crypt depth ratio was subsequently calculated.

Western Blotting

Western blot analysis was used to examine protein expression in THP-1 cells and mouse ileal tissues. In brief, cell or tissue samples were lysed with RIPA buffer supplemented with 1% PMSF and incubated on ice for 30 min. Cell lysates were centrifuged at 12,000 rpm for 15 min to remove insoluble debris, and the clarified supernatants were harvested for subsequent assays. Protein concentrations were measured with a BCA protein assay kit obtained from Epizyme (Shanghai, China). An equal amount of protein from each sample (20–30 μg/lane) was subjected to SDS-PAGE, followed by transfer onto PVDF membranes. The membranes were blocked with 5% BSA for 1 h at room temperature and incubated with the indicated primary antibodies overnight at 4°C against NLRP3, GSDMD, ASC, Caspase-1, IL-1β, and β-actin. β-actin was used as the internal loading control. After overnight primary antibody incubation, membranes were washed three times with Tris-buffered saline containing Tween-20 (TBST) for 10 min per wash, followed by incubation with corresponding secondary antibodies for 1 h at room temperature. After incubation with secondary antibodies, the membranes were rinsed three times with TBST. Immunoreactive bands were then visualized using a Tanon chemiluminescence detection system, and grayscale analysis was performed using ImageJ software for semi-quantitative analysis.

Real-Time Quantitative PCR Assay

Total RNA from THP-1 cells and mouse ileal tissues was extracted with the FastPure Cell/Tissue Total RNA Isolation Kit (Vazyme, Nanjing, China) following the manufacturer's protocol. The isolated RNA was then reverse-transcribed into cDNA for subsequent real-time quantitative PCR analysis. Relative mRNA levels were calculated by the 2^−ΔΔCt method, using GAPDH as the internal control. The primers for target genes were designed and synthesized by Shanghai Generay Biotech Co., Ltd., and their sequences are provided in Supplementary Table 1. All experiments were performed at least three times, with each sample analyzed in triplicate.

Statistical Analysis

Data are presented as the mean ± SD. For comparisons involving more than two groups, one-way ANOVA followed by Tukey's multiple-comparison test was applied. A value of $P < 0.05$ was considered statistically significant. All experiments were conducted independently at least three times. Statistical analyses and graph generation were performed with GraphPad Prism 10.0.

Results

ω-3 PUFAs Ameliorated Ileal Tissue Injury and Improved Smooth Muscle Function-Related Markers in POI Mice

HE staining showed that the ileal villi in the Sham group were intact and regularly arranged, with clearly defined crypt structures and no obvious inflammatory cell infiltration. In contrast, mice in the POI group exhibited markedly shortened and disorganized ileal villi, accompanied by mucosal structural injury and varying degrees of inflammatory cell infiltration in the mucosal and submucosal layers (Fig. 1A).

Compared with the POI group, ω-3 PUFA treatment significantly increased villus height and the villus height/crypt depth (V/C) ratio, while markedly reducing the histological injury score, indicating that ω-3 PUFAs effectively alleviated POI-associated intestinal morphological damage (Fig. 1C, E, F).

To further evaluate changes in intestinal smooth muscle function, the mRNA expression levels of smooth muscle function-related markers were examined. RT-qPCR analysis showed that the mRNA levels of MLC and α-SMA were significantly decreased in the POI group compared with the Sham group. After ω-3 PUFA intervention, the expression levels of both markers were significantly upregulated in a dose-dependent manner, suggesting that ω-3 PUFAs promoted the recovery of intestinal smooth muscle function-related markers in POI mice (Fig. 1B, D).

Proteomic Analysis Identified Potential Signaling Pathways Involved in the Protective Effects of ω-3 PUFAs Against POI

To explore the potential molecular mechanisms by which ω-3 PUFAs ameliorate POI, quantitative proteomic analysis was performed on ileal tissues from mice in the Sham, POI, and ω-3 PUFA-treated groups (Fig. 2). Principal component analysis (PCA) showed a clear separation trend among the groups based on their overall protein expression profiles, indicating that both POI modeling and ω-3 PUFA intervention substantially altered the proteomic landscape of ileal tissues (Fig. 2A).

Proteomic profiling identified 746 upregulated and 270 downregulated proteins in the POI group compared with the Sham group. In contrast, ω-3 PUFA treatment altered the expression of 1,370 proteins relative to the POI group, including 758 upregulated and 612 downregulated proteins (Fig. 2B, C), suggesting that ω-3 PUFAs markedly remodeled the aberrant protein expression pattern induced by POI.

Further KEGG enrichment and GSEA analyses [26–27] revealed that the differentially expressed proteins were significantly enriched in the NOD-like receptor signaling pathway. This pathway is closely associated with inflammasome activation, inflammatory cytokine maturation, and pyroptosis [17–21, 25]. Assembly of the NLRP3 inflammasome represents a central event in this pathway. Once activated, inflammasome activation facilitates the processing and secretion of inflammatory mediators, including IL-1β and IL-18, and induces GSDMD-dependent pyroptosis. Clustered heatmap analysis showed that inflammasome-related proteins, including NLRP3, Caspase-1, Pycard/ASC, IL-1β, IL-18, and GSDMD, were generally upregulated in the POI group, whereas their expression levels were markedly reduced following ω-3 PUFA intervention (Fig. 2D–G). These results suggest that the NOD-like receptor/NLRP3 inflammasome pathway may serve as an important target through which ω-3 PUFAs alleviate intestinal inflammation in POI.

ω-3 PUFAs Suppressed NLRP3, ASC, and IL-1β Expression in Ileal Tissues of POI Mice

The expression of inflammasome-related proteins in ileal tissues was further examined by immunohistochemistry (Fig. 3A-C). The ileal tissues of POI mice displayed a markedly higher percentage

of NLRP3, ASC, and IL-1β-positive cells than those of Sham mice, indicating that POI induced pronounced inflammasome activation and inflammatory responses. After treatment with different doses of ω-3 PUFAs, these inflammatory markers showed a dose-dependent decreasing trend.

Compared with the POI group, low-dose ω-3 PUFA treatment significantly reduced the proportion of NLRP3-, ASC-, and IL-1β-positive cells, while medium- and high-dose ω-3 PUFA treatment further suppressed the expression of these markers, with the high-dose group showing the most prominent inhibitory effect (Fig. 3D–F). These quantitative results demonstrate that ω-3 PUFAs significantly inhibit POI-induced expression of inflammasome-related proteins, suggesting that ω-3 PUFAs may alleviate postoperative intestinal inflammation and promote intestinal functional recovery by negatively regulating the NLRP3/ASC/IL-1β inflammatory pathway.

ω-3 PUFAs inhibited activation of the NLRP3/Caspase-1/GSDMD pyroptotic signaling pathway in the ileum of POI mice

To systematically evaluate the regulatory effects of ω-3 PUFAs on inflammasome activation and pyroptosis-related signaling in postoperative ileus, Western blot analysis was performed using ileal tissues from mice (Fig. 4). Compared with the Sham group, the POI group showed markedly upregulated expression of NLRP3, ASC, Caspase-1, cleaved Caspase-1 p20, GSDMD, and IL-1β, indicating pronounced activation of inflammasome-related signaling and inflammatory mediator release in the ileal muscularis. In contrast, ω-3 PUFA treatment significantly reduced the expression of these proteins. Semiquantitative analysis further showed that their expression levels were restored toward those observed in the Sham group, suggesting that ω-3 PUFAs effectively suppressed inflammasome activation and GSDMD-mediated pyroptotic signaling in POI (Fig. 4A–B).

These findings were consistent with the proteomic analysis, in which differentially expressed proteins were mainly associated with NOD-like receptor signaling, further supporting the critical involvement of the NLRP3 inflammasome in POI-associated intestinal inflammatory responses. RT-qPCR was subsequently performed to assess the mRNA expression of inflammasome-related genes. Relative to the Sham group, the POI group showed a marked increase in mRNA levels of ASC, NLRP3, IL-1β, and Caspase-1. Following ω-3 PUFA intervention, the expression levels of these genes were markedly downregulated, with the high-dose group showing a stronger inhibitory effect than the low-dose group (Fig. 4C-F).

Collectively, these results demonstrate that POI is associated with robust activation of the NLRP3 inflammasome and enhanced pyroptosis-related signaling in ileal tissues. ω-3 PUFAs attenuated this response through reduced NLRP3 and ASC expression together with impaired Caspase-1 activation, reducing IL-1β maturation and release, and limiting GSDMD-mediated pyroptotic signaling. These findings support a protective role of ω-3 PUFAs in POI, potentially through suppression of the NLRP3/Caspase-1/GSDMD signaling pathway.

ω-3 PUFAs regulated macrophage infiltration and M1/M2 polarization in the ileum of POI mice

To further clarify the effects of ω-3 PUFAs on intestinal macrophage infiltration and polarization in POI mice, triple immunofluorescence staining was performed to detect F4/80, CD86, and CD206 expression.

Compared with the Sham group, the POI group exhibited markedly enhanced F4/80 and CD86 fluorescence signals in ileal tissues, accompanied by decreased CD206 expression. These findings indicate that POI induced macrophage infiltration and facilitated the shift of macrophages toward an M1-like pro-inflammatory phenotype. After ω-3 PUFA treatment, F4/80 and CD86 expression were notably reduced, whereas CD206 expression was increased, with the most evident effects observed in the medium- and high-dose groups (Fig. 5).

Collectively, these observations suggest that ω-3 PUFAs reduced macrophage infiltration in the ileum of POI mice, inhibited pro-inflammatory M1 macrophage polarization, and promoted the transition toward an immunoregulatory and reparative M2 phenotype, thereby contributing to the alleviation of POI-associated intestinal inflammation.

ω-3 PUFAs suppressed inflammasome activation and inflammatory responses in macrophages

To validate the regulatory effects of ω-3 PUFAs on inflammasome activation and macrophage polarization, an inflammasome activation model established by LPS/ATP stimulation model was established in THP-1 cells [17–19, 23]. CCK-8 assays showed that treatment with 100 μM EPA or 100 μM DHA for 24 h did not affect cell viability, indicating that the selected concentrations were not cytotoxic.

Western blot analysis showed that, compared with the control group, the model group exhibited significantly increased protein expression levels of NLRP3, ASC, Caspase-1, cleaved Caspase-1 p20, GSDMD, and IL-1β. However, ω-3 PUFA treatment markedly reduced the expression of these proteins in a dose-dependent manner. ELISA further confirmed that IL-1β secretion was significantly elevated in the model group compared with the control group, whereas ω-3 PUFA intervention significantly decreased IL-1β levels. Notably, the inhibitory effect observed in the high-dose ω-3 PUFA group was comparable to that of the NLRP3 inhibitor MCC950 [24], suggesting a potent anti-inflammatory effect of ω-3 PUFAs.

Meanwhile, IL-10, an anti-inflammatory cytokine, was markedly reduced in the model group than in the control group, whereas ω-3 PUFA treatment markedly increased IL-10 secretion. This effect was most evident in the high-dose group. MCC950 treatment also significantly increased IL-10 levels, further supporting the role of ω-3 PUFAs in promoting an anti-inflammatory macrophage response.

To visually assess the effects of ω-3 PUFAs on NLRP3 inflammasome assembly in macrophages, immunofluorescence colocalization staining was performed to detect the expression of NLRP3 and ASC in THP-1 cells. As shown in Fig. 6, NLRP3 and ASC fluorescence signals were relatively weak in the

control group, with limited colocalization. Following LPS/ATP stimulation, both NLRP3 and ASC expression were markedly enhanced, accompanied by obvious fluorescence overlap, indicating increased inflammasome assembly.

Pretreatment with ω-3 PUFAs substantially attenuated NLRP3 and ASC fluorescence signals and reduced their colocalization, with the high-dose group showing the most pronounced inhibitory effect. This trend was consistent with that observed in the MCC950-treated group. Collectively, these findings indicate that ω-3 PUFAs suppressed inflammasome activation induced by LPS/ATP.NLRP3 inflammasome assembly and pyroptotic pathway activation in macrophages while modulating macrophage polarization toward an anti-inflammatory phenotype.

ω-3 PUFAs Inhibited LPS/ATP-Induced NLRP3 Inflammasome Activation in THP-1-Derived Macrophages

To investigate the effects of ω-3 PUFAs on pyroptosis-related inflammatory responses in macrophages, THP-1-derived macrophages were stimulated with LPS/ATP to establish an M1-like inflammatory model. The abundance of proteins associated with NLRP3 inflammasome activation and genes were then examined (Fig. 7).

Western blotting showed that, compared with the Control group, the expression levels of NLRP3, ASC, cleaved Caspase-1 p20 and p10, mature IL-1β, and the pyroptosis executioner protein GSDMD-N were significantly increased in the M1 group. These findings indicated that LPS/ATP successfully activated the NLRP3 inflammasome and induced pyroptosis in THP-1-derived macrophages. Relative to the M1 group, ω-3 PUFA administration markedly reduced the expression of these proteins, with the high-dose group (ω3-H) showing a stronger inhibitory effect than the low-dose group (ω3-L). Similarly, treatment with MCC950, a specific NLRP3 inhibitor, markedly reduced the levels of NLRP3, ASC, GSDMD-N, Caspase-1 p20/p10, and IL-1β (Fig. 7A–B).

RT-qPCR was further performed to detect the mRNA expression levels of related genes. The results showed that the mRNA levels of NLRP3, ASC, Caspase-1, and IL-1β were significantly increased in the M1 group compared with the Control group. After ω-3 PUFA intervention, the expression levels of these genes were markedly decreased, with a greater reduction observed in the high-dose group. MCC950 treatment also exerted a significant inhibitory effect (Fig. 7C–F).

Together, these data indicate that ω-3 PUFAs suppress NLRP3 inflammasome activation induced by LPS/ATP in THP-1-derived macrophages, reduce Caspase-1 activation and GSDMD-mediated pyroptosis, and decrease the production of mature IL-1β. The regulatory pattern of ω-3 PUFAs was similar to that of the specific NLRP3 inhibitor MCC950, suggesting that ω-3 PUFAs may attenuate inflammatory responses through inhibition of the NLRP3/Caspase-1/GSDMD signaling cascade.

Discussion

POI is a common functional gastrointestinal motility disorder following abdominal surgery, and its occurrence and progression are closely associated with inflammatory responses within the intestinal muscularis [28]. Previous studies have shown that surgical manipulation can induce intestinal tissue injury and activate the local immune system, particularly resident macrophages in the intestinal muscularis, leading to the release of multiple inflammatory mediators and delayed recovery of gastrointestinal motility [29]. In the present study, we found that POI was accompanied by markedly elevated intestinal inflammation and upregulated expression of molecules linked to activation of the NLRP3/Caspase-1/IL-1β inflammatory cascade.ω-3 PUFA intervention significantly reversed these changes, suggesting a protective role of ω-3 PUFAs in POI.

The NLRP3 inflammasome is an important intracellular inflammatory signaling complex, and its activation generally requires two steps: priming and activation. Damage-associated molecular patterns (DAMPs) released after surgical injury can activate the NF-κB signaling pathway, leading to elevated expression of NLRP3 and pro-IL-1β. Subsequently, ATP, reactive oxygen species (ROS), and other danger signals further induce NLRP3 inflammasome assembly, promote Caspase-1 cleavage and activation, and ultimately convert pro-IL-1β into mature IL-1β, thereby amplifying inflammatory responses [17–21, 25]. In this study, the expression levels of NLRP3, Caspase-1, and IL-1β were significantly increased in the POI model group, indicating activation of the inflammasome pathway. In contrast, ω-3 PUFA treatment markedly reduced the expression of these key molecules, suggesting that ω-3 PUFAs exert anti-inflammatory effects by inhibiting NLRP3 inflammasome activation.

Of note, our previous research indicated that ω-3 PUFAs could mitigate intestinal inflammation in POI by downregulating the JAK2/STAT3 signaling pathway and regulating macrophage M1/M2 polarization [30]. On this basis, Our results further indicate that the inflammation-resolving actions of ω-3 PUFAs are not merely attributable to reduced inflammatory cytokine expression, but may also involve regulation of the entire process of inflammasome activation. On the one hand, ω-3 PUFAs may reduce NF-κB pathway activity, thereby lowering NLRP3 and pro-IL-1β expression and limiting the molecular basis required for inflammasome activation and decreasing the molecular substrates required for inflammasome activation [31]. On the other hand, ω-3 PUFAs may suppress NLRP3 inflammasome assembly and Caspase-1 activation by modulating cell membrane lipid composition, reducing ROS production, and improving mitochondrial function, ultimately decreasing the generation and release of mature IL-1β. These multilevel regulatory effects collectively contribute to the overall anti-inflammatory actions of ω-3 PUFAs [32].

In addition to inflammasome signaling, macrophage polarization contributes substantially to POI pathogenesis. M1-polarized macrophages typically produce high levels of pro-inflammatory mediators, such as IL-1β, TNF-α, and IL-18,which can aggravate inflammatory responses and inhibit intestinal smooth muscle contractility. In contrast, M2-like macrophages are involved in inflammation resolution and tissue repair. In the present study, POI was associated with an enhanced pro-inflammatory microenvironment, suggesting a predominance of M1-like macrophage responses. After ω-3 PUFA

intervention, inflammatory levels were reduced, indicating that ω-3 PUFAs may promote the transition of macrophages from a pro-inflammatory state to an anti-inflammatory and tissue-repair phenotype [33–36]. These findings further suggest that the protective effects of ω-3 PUFAs are not restricted to the inhibition of a single molecular target, but instead involve broader regulation of the immune microenvironment within the intestinal muscularis.

From a functional perspective, enhanced inflammatory responses directly impair the recovery of intestinal motility. Pro-inflammatory mediators such as IL-1β may upregulate iNOS expression, thereby increasing nitric oxide and prostaglandin E_2 (PGE_2) production,thereby reducing smooth muscle contractility and ultimately weakening gastrointestinal peristalsis. In this study, intestinal transit was markedly impaired in the POI model group, whereas ω-3 PUFA treatment significantly improved intestinal transport capacity. This improvement was accompanied by decreased inflammatory responses and inhibition of the NLRP3 inflammasome pathway, suggesting that inflammasome-mediated inflammation plays a critical role in POI-related gastrointestinal dysmotility and that ω-3 PUFAs facilitate gastrointestinal functional recovery by suppressing this process [37–39].

Proteomic profiling showed that the differentially expressed proteins were markedly enriched in the NOD-like receptor signaling pathway, supporting the rationale for investigating the NLRP3 inflammasome in this study. Nevertheless, this pathway includes various NOD-like receptors and downstream immune-related molecules. Thus, although our results provide strong evidence for the potential implication of the NLRP3 inflammasome, the participation of other inflammasome complexes or associated innate immune signaling pathways cannot be entirely ruled out.

Collectively, our findings demonstrate that ω-3 PUFAs alleviate POI-associated inflammatory injury and promote the recovery of gastrointestinal motility by inhibiting activation of the NLRP3/Caspase-1/IL-1β inflammatory pathway, reducing pyroptosis, regulating macrophage polarization, and improving the immune microenvironment within the intestinal muscularis. Together with our previous findings regarding the JAK2/STAT3 signaling pathway, these results suggest that ω-3 PUFAs may exert anti-inflammatory effects through coordinated regulation of multiple pathways and targets. This study not only further enriches the understanding of inflammatory and immune mechanisms underlying POI, but also provides mechanistic support for the application of ω-3 PUFAs in perioperative nutritional intervention and POI prevention and treatment.

Conclusion

The current study provided a comprehensive assessment of the protective effects of ω-3 PUFAs against POI and explored their potential underlying mechanisms. The results demonstrated that ω-3 PUFAs mitigated intestinal inflammatory responses and improved gastrointestinal motility recovery, potentially through suppression of the NLRP3/Caspase-1/IL-1β inflammatory axis in intestinal muscularis macrophages and regulating macrophage polarization. Evidence from both animal and cellular experiments demonstrated that ω-3 PUFAs improved inflammatory cytokine expression, intestinal tissue

architecture, and intestinal transit function. These findings provide novel molecular targets and a theoretical foundation for developing preventive and therapeutic strategies against POI. Future studies incorporating clinical samples are warranted to further validate the safety and efficacy of ω-3 PUFAs in clinical practice.

Declarations

Acknowledgments

We thank the animal facility staff for their assistance with animal care and the laboratory technical staff for their support during the experiments.

Author Contributions

Liuchuang Zhang (First Author) and Haoran Gu (Co-first Author): Conceptualization, Data Curation, Formal Analysis, Investigation, Methodology, Software, Visualization, Writing-Original Draft, Writing-Review & Editing; Gang Wang and Zhiwei Jiang (Corresponding Author): Conceptualization, Funding Acquisition, Resources, Supervision, Validation, Writing-Original Draft, Writing-Review & Editing; Jing Yu: Methodology, Supervision; Writing-Review & Editing Xuan Zhao: Supervision, Validation; Writing-Review & Editing Yiting Li: Data Curation, Supervision; Writing-Review & Editing Huafeng Pan: Resources; Supervision; Writing-Review & Editing Haifeng Wang: Resources; Validation; Writing-Review & Editing Miaomiao Ge: Investigation; Supervision; Writing-Review & Editing All authors took part in drafting, revising or critically reviewing the article; gave final approval of the version to be published; have agreed on the journal to which the article has been submitted; and agree to be accountable for all aspects of the work."

Funding

This work was supported by the Jiangsu Provincial Key Discipline Project (ZDXK202251), Jiangsu Provincial,Association of Chinese Medicine Revitalization and Development Project (ZXFZ2024001), and Jiangsu Postgraduate

ARRIVE Guidelines Statement

This study was designed, conducted, and reported in strict accordance with the ARRIVE guidelines (Animal Research: Reporting of In Vivo Experiments). All animal experiments were performed using male C57BL/6 mice. The mice were randomly assigned to experimental groups, with a defined sample size of 10 mice per group. The experimental procedures, including preoperative preparation, anesthesia, surgical manipulation, and postoperative care, were conducted in a specific pathogen-free facility according to standard operating procedures. All euthanasia procedures complied with ethical requirements and were approved by the Ethics Committee of the Affiliated Hospital of Nanjing University of Chinese Medicine (Approval No. 2026DW-084-01). During the experimental period, the health status, body weight, and

physiological parameters of the mice were monitored, and all experimental data were recorded to ensure the reproducibility and scientific validity of the results.

Declaration of generative AI and AI-assisted technologies in the manuscript preparation process

During the preparation of this manuscript, the authors used ChatGPT (OpenAI) to assist with drafting selected passages, translation, and language editing. All AI-assisted text was subsequently reviewed and revised by the authors, who take full responsibility for the accuracy, integrity, and final content of the manuscript.

Data Availability Statement

All data generated or analyzed during this study are included in this published article and its supplementary materials. Additional data are available from the corresponding author upon reasonable request.

Conflicts of Interest and Funding Statement

The authors declare that they have no conflicts of interest.

Funding information should be added here if applicable.

Disclosure

No potential competing interest was reported by the authors.

References

1. Vather R, Trivedi S, Bissett I. Defining postoperative ileus: results of a systematic review and global survey. J Gastrointest Surg. 2013;17(5):962–972. doi:10.1007/s11605-013-2148-y
2. Bragg D, El-Sharkawy AM, Psaltis E, et al. Postoperative ileus: recent developments in pathophysiology and management. Clin Nutr. 2015;34(3):367–376. doi:10.1016/j.clnu.2015.01.016
3. Chapman SJ, Pericleous A, Downey C, et al. Postoperative ileus following major colorectal surgery. Br J Surg. 2018;105(7):797–810. doi:10.1002/bjs.10854
4. Vilz TO, Stoffels B, Strassburg C, et al. Ileus in adults: pathogenesis, investigation and treatment. Dtsch Arztebl Int. 2017;114(29-30):508–517. doi:10.3238/arztebl.2017.0508
5. Venara A, Neunlist M, Slim K, et al. Postoperative ileus: pathophysiology, incidence, and prevention. J Visc Surg. 2016;153(6):439–446. doi:10.1016/j.jviscsurg.2016.08.010
6. Calder PC. Omega-3 fatty acids and inflammatory processes: from molecules to man. Biochem Soc Trans. 2017;45(5):1105–1115. doi:10.1042/BST20160474
7. Serhan CN, Chiang N, Van Dyke TE. Resolving inflammation: dual anti-inflammatory and pro-resolution lipid mediators. Nat Rev Immunol. 2008;8(5):349–361. doi:10.1038/nri2294

8. Oh DY, Talukdar S, Bae EJ, et al. GPR120 is an omega-3 fatty acid receptor mediating potent anti-inflammatory and insulin-sensitizing effects. Cell. 2010;142(5):687–698. doi:10.1016/j.cell.2010.07.041
9. Kalff JC, Carlos TM, Schraut WH, et al. Surgically induced leukocytic infiltrates within the rat intestinal muscularis mediate postoperative ileus. Gastroenterology. 1999;117(2):378–387. doi:10.1053/gast.1999.0029900378
10. Wehner S, Behrendt FF, Lyutenski BN, et al. Inhibition of macrophage function prevents intestinal inflammation and postoperative ileus in rodents. Gut. 2007;56(2):176–185. doi:10.1136/gut.2005.089615
11. de Jonge WJ, van den Wijngaard RM, The FO, et al. Postoperative ileus is maintained by intestinal immune infiltrates that activate inhibitory neural pathways in mice. Gastroenterology. 2003;125(4):1137–1147. doi:10.1016/S0016-5085(03)01197-1
12. Stoffels B, Hupa KJ, Snoek SA, et al. Postoperative ileus involves interleukin-1 receptor signaling in enteric glia. Gastroenterology. 2014;146(1):176–187.e1. doi:10.1053/j.gastro.2013.09.030
13. Hupa KJ, Stein K, Schneider R, et al. AIM2 inflammasome-derived IL-1β induces postoperative ileus in mice. Sci Rep. 2019;9(1):10602. doi:10.1038/s41598-019-46968-1
14. Martinon F, Burns K, Tschopp J. The inflammasome: a molecular platform triggering activation of inflammatory caspases and processing of proIL-β. Mol Cell. 2002;10(2):417–426. doi:10.1016/S1097-2765(02)00599-3
15. Broz P, Dixit VM. Inflammasomes: mechanism of assembly, regulation and signalling. Nat Rev Immunol. 2016;16(7):407–420. doi:10.1038/nri.2016.58
16. He Y, Hara H, Núñez G. Mechanism and regulation of NLRP3 inflammasome activation. Trends Biochem Sci. 2016;41(12):1012–1021. doi:10.1016/j.tibs.2016.09.002
17. Shi J, Zhao Y, Wang K, et al. Cleavage of GSDMD by inflammatory caspases determines pyroptotic cell death. Nature. 2015;526(7575):660–665. doi:10.1038/nature15514
18. Ramachandran R, Manan A, Kim J, et al. NLRP3 inflammasome: a key player in the pathogenesis of lifestyle disorders. Exp Mol Med. 2024;56:1488–1500. doi:10.1038/s12276-024-01261-8
19. Yang S, Li W, Bai X, et al. Ginseng-derived nanoparticles alleviate inflammatory bowel disease via the TLR4/MAPK and p62/Nrf2/Keap1 pathways. J Nanobiotechnology. 2024;22(1):48. doi:10.1186/s12951-024-02313-x
20. Ouagueni A, Al-Zoubi RM, Zarour A, et al. Effects of omega-3 polyunsaturated fatty acids, docosahexaenoic acid and eicosapentaenoic acid, on post-surgical complications in trauma patients: mechanisms, nutrition, and challenges. Mar Drugs. 2024;22(5):207. doi:10.3390/md22050207
21. Hudert CA, Weylandt KH, Lu Y, et al. Transgenic mice rich in endogenous omega-3 fatty acids are protected from colitis. Proc Natl Acad Sci U S A. 2006;103(30):11276–11281. doi:10.1073/pnas.0601280103

22. Tian D, Liu B, Huang S, et al. Postoperative Ileus Murine Model. J Vis Exp. 2024;(209):e66465. doi:10.3791/66465
23. Genin M, Clement F, Fattaccioli A, et al. M1 and M2 macrophages derived from THP-1 cells differentially modulate the response of cancer cells to etoposide. BMC Cancer. 2015;15:577. doi:10.1186/s12885-015-1546-9
24. Coll RC, Robertson AAB, Chae JJ, et al. A small-molecule inhibitor of the NLRP3 inflammasome for the treatment of inflammatory diseases. Nat Med. 2015;21(3):248–255. doi:10.1038/nm.3806
25. Swanson KV, Deng M, Ting JP-Y. The NLRP3 inflammasome: molecular activation and regulation to therapeutics. Nat Rev Immunol. 2019;19(8):477–489. doi:10.1038/s41577-019-0165-0
26. Subramanian A, Tamayo P, Mootha VK, et al. Gene set enrichment analysis: a knowledge-based approach for interpreting genome-wide expression profiles. Proc Natl Acad Sci U S A. 2005;102(43):15545–15550. doi:10.1073/pnas.0506580102
27. Kanehisa M, Goto S. KEGG: Kyoto Encyclopedia of Genes and Genomes. Nucleic Acids Res. 2000;28(1):27–30. doi:10.1093/nar/28.1.27
28. Luckey A, Livingston E, Taché Y. Mechanisms and treatment of postoperative ileus. Arch Surg. 2003;138(2):206–214. doi:10.1001/archsurg.138.2.206
29. Enderes J, Schneider R, Hupa KJ, et al. A population of radio resistant macrophages in the deep myenteric plexus contributes to postoperative ileus via Toll like receptor 3 signaling. Front Immunol. 2021;11:581111. doi:10.3389/fimmu.2020.581111
30. Zhao X, Yu J, Zhang T, et al. ω-3 PUFAs attenuate postoperative ileus by modulating macrophage polarization via the JAK2/STAT3 signaling pathway. J Inflamm Res. 2026;19:562643. doi:10.2147/JIR.S562643
31. Calder PC. Marine omega-3 fatty acids and inflammatory processes: Effects, mechanisms and clinical relevance. Biochim Biophys Acta Mol Cell Biol Lipids. 2015;1851(4):469–484. doi:10.1016/j.bbalip.2014.08.010
32. Yan Y, Jiang W, Spinetti T, et al. Omega-3 fatty acids prevent inflammation and metabolic disorder through inhibition of NLRP3 inflammasome activation. Immunity. 2013;38(6):1154–1163. doi:10.1016/j.immuni.2013.05.015
33. Calder PC, Bosco N, Bourre J, et al. n-3 Fatty acids, inflammation and immunity: New mechanisms to explain old actions. Proc Nutr Soc. 2013;72(3):326–336. doi:10.1017/S0029665113001031
34. Murray PJ, Allen JE, Biswas SK, et al. Macrophage activation and polarization: nomenclature and experimental guidelines. Immunity. 2014;41(1):14–20. doi:10.1016/j.immuni.2014.06.008
35. Sica A, Mantovani A. Macrophage plasticity and polarization: in vivo veritas. J Clin Invest. 2012;122(3):787–795. doi:10.1172/JCI59643
36. Mosser DM, Edwards JP. Exploring the full spectrum of macrophage activation. Nat Rev Immunol. 2008;8(12):958–969. doi:10.1038/nri2448

37. Bauer AJ, Schwarz NT, Moore BA, et al. Ileus in critical illness: mechanisms and management. Curr Opin Crit Care. 2002;8(2):152–157. doi:10.1097/00075198-200204000-00011
38. Boeckxstaens GE, de Jonge WJ, De Schepper HU, et al. Neuroimmune mechanisms in postoperative ileus. Gut. 2009;58(9):1300–1311. doi:10.1136/gut.2008.169250
39. Docsa T, Sipos A, Cox CS, et al. The Role of Inflammatory Mediators in the Development of Gastrointestinal Motility Disorders. Int J Mol Sci. 2022;23(13):6917. doi:10.3390/ijms23136917
40. Watanabe D, Guo Y, Kamada N, et al. Interaction between the inflammasome and commensal microorganisms in gastrointestinal health and disease. EMBO Mol Med. 2021;13:e13452. doi:10.15252/emmm.202013452

Figures

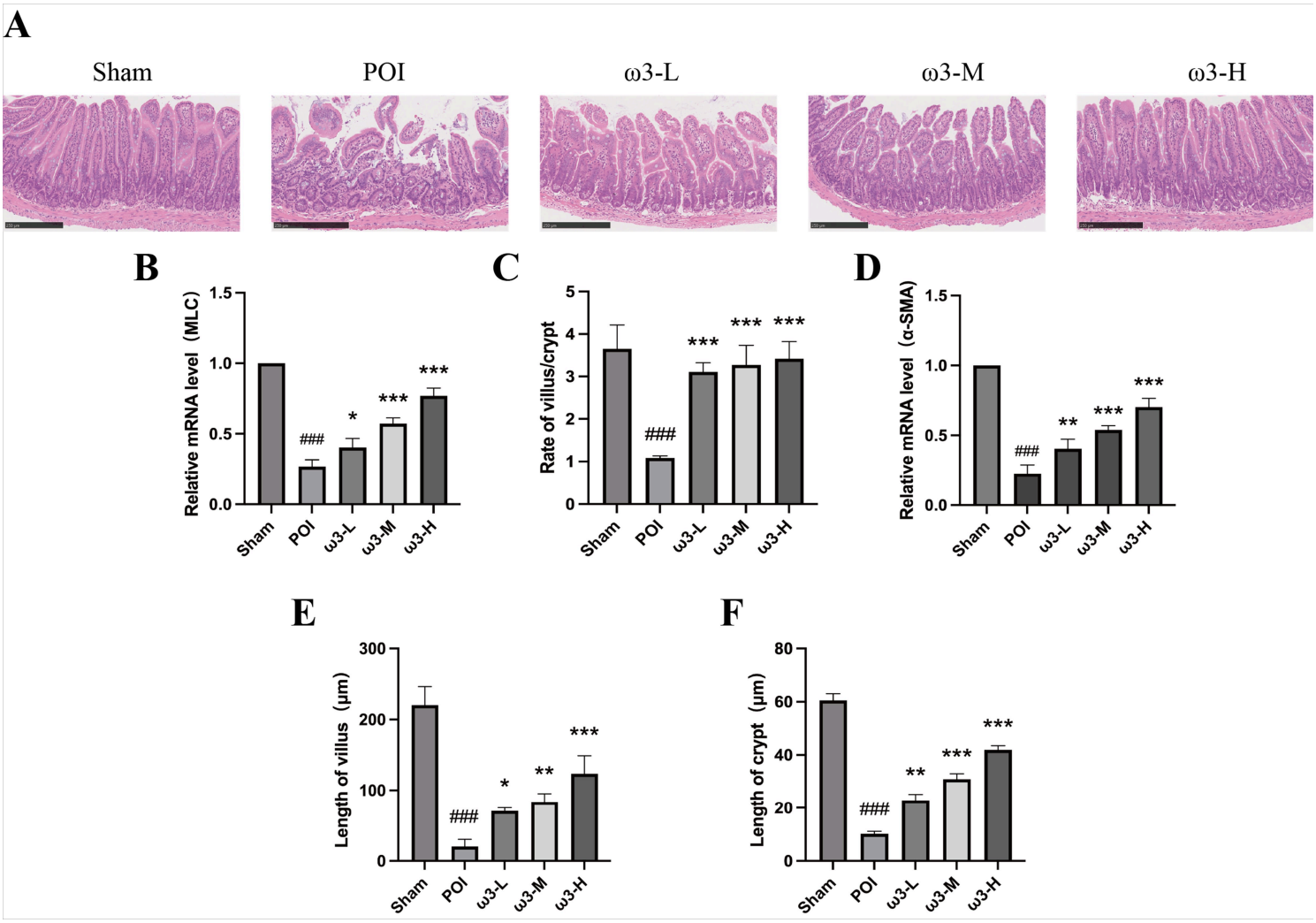


Figure 1

ω-3 PUFAs attenuated ileal injury and improved intestinal morphology in POI mice.(**A**) Representative HE-stained images of ileal tissues from each group (scale bar = 100 μm, n = 6). (**B and D**) Relative mRNA expression of MLC and α-SMA detected by RT-qPCR (n = 6). (**C**) Villus height/crypt depth ratio (n = 6). (**E**

and F) Quantification of villus length and crypt depth, respectively (n = 6). Data are presented as the mean ± SD. ###P < 0.001 vs. Sham; *P < 0.05, **P < 0.01, ***P < 0.001 vs. POI.

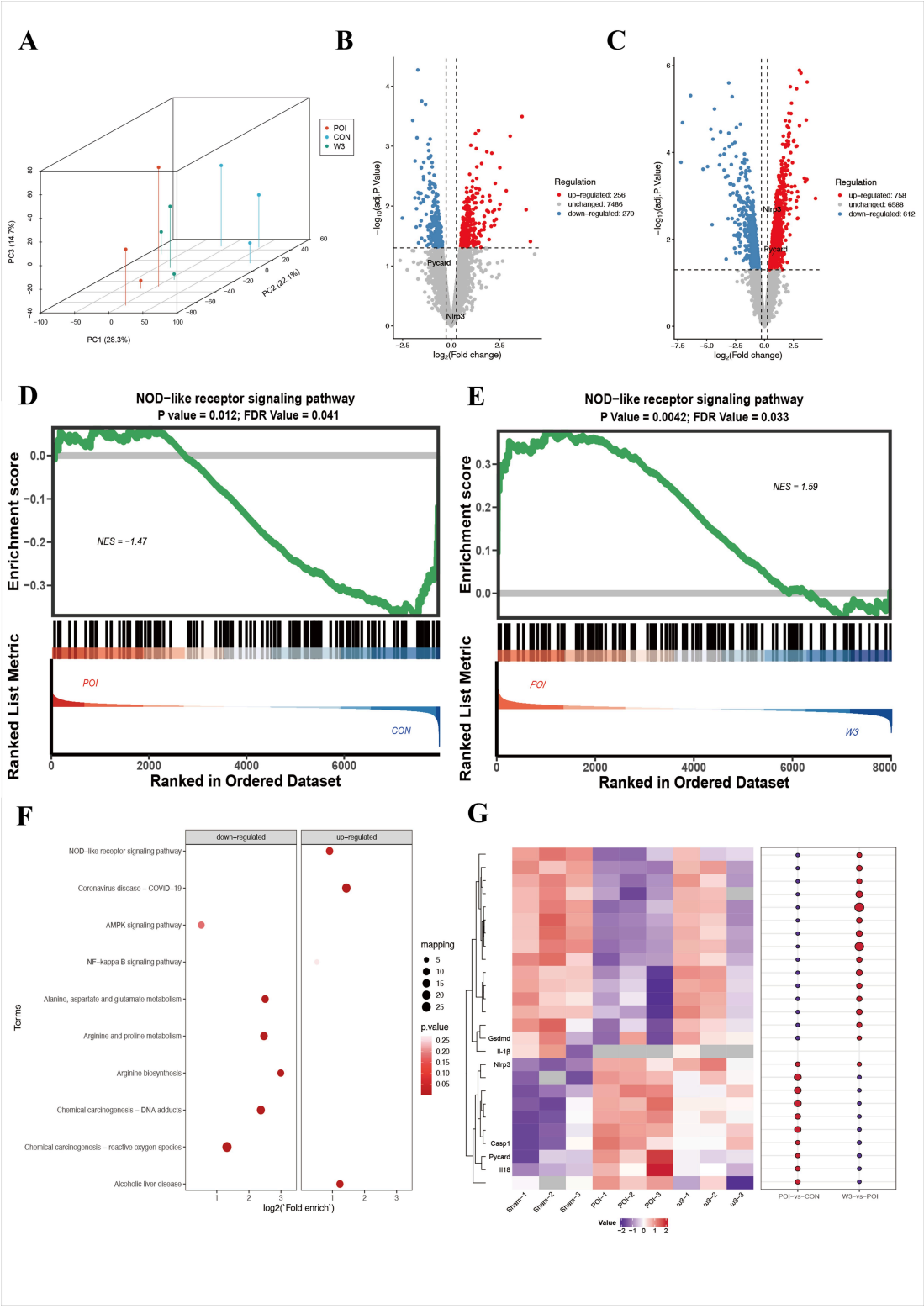


Figure 2

Proteomic analysis identified activation of the NOD-like receptor signaling pathway in POI mice.(**A**) PCA of protein expression profiles among the Sham, POI, and ω-3 PUFA-treated groups. (**B and C**)

Volcano plots of differentially expressed proteins in the POI versus Sham and ω-3 PUFA-treated versus POI comparisons, respectively. (**D and E**) GSEA of the NOD-like receptor signaling pathway. (**F**) KEGG enrichment analysis of differentially expressed proteins. (**G**) Heatmap of inflammasome- and pyroptosis-related proteins across different groups.

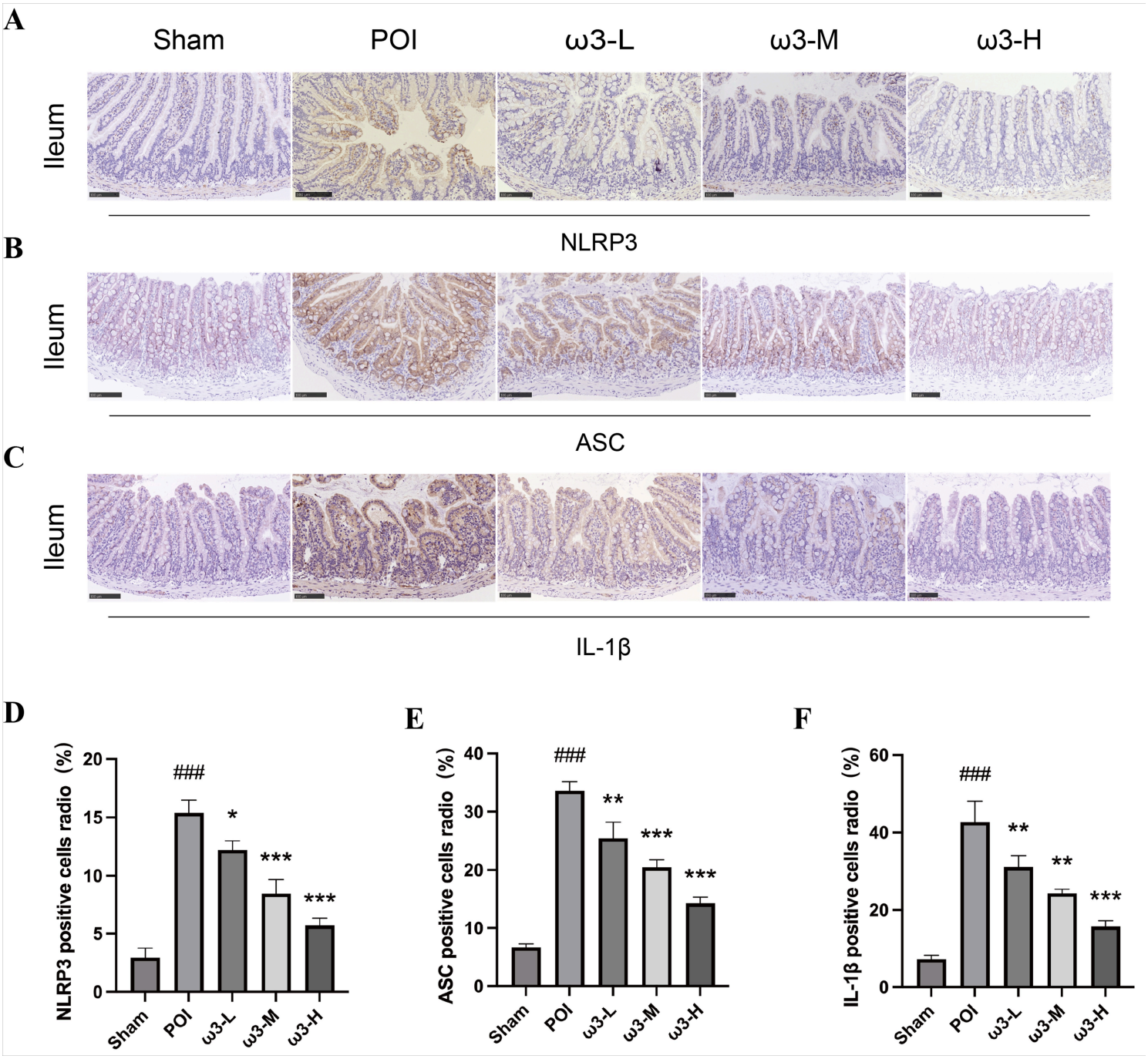


Figure 3

ω-3 PUFAs suppressed NLRP3 inflammasome-related protein expression in the ileum of POI mice.(**A–C**) Representative immunohistochemical staining images of NLRP3, ASC, and IL-1β in ileal tissues from the Sham, POI, ω3-L, ω3-M, and ω3-H groups, respectively (scale bar = 100 μm, n = 3). Compared with the Sham group, POI mice exhibited markedly increased positive staining for NLRP3, ASC, and IL-1β in

ileal tissues, whereas ω-3 PUFA treatment reduced the expression of these proteins in a dose-dependent manner. (**D–F**) Quantitative analysis of the positive staining ratios of NLRP3, ASC, and IL-1β, respectively (n = 3). Data are presented as the mean ± SD. ###P < 0.001 vs. Sham group; *P < 0.05, **P < 0.01, ***P < 0.001 vs. POI group.

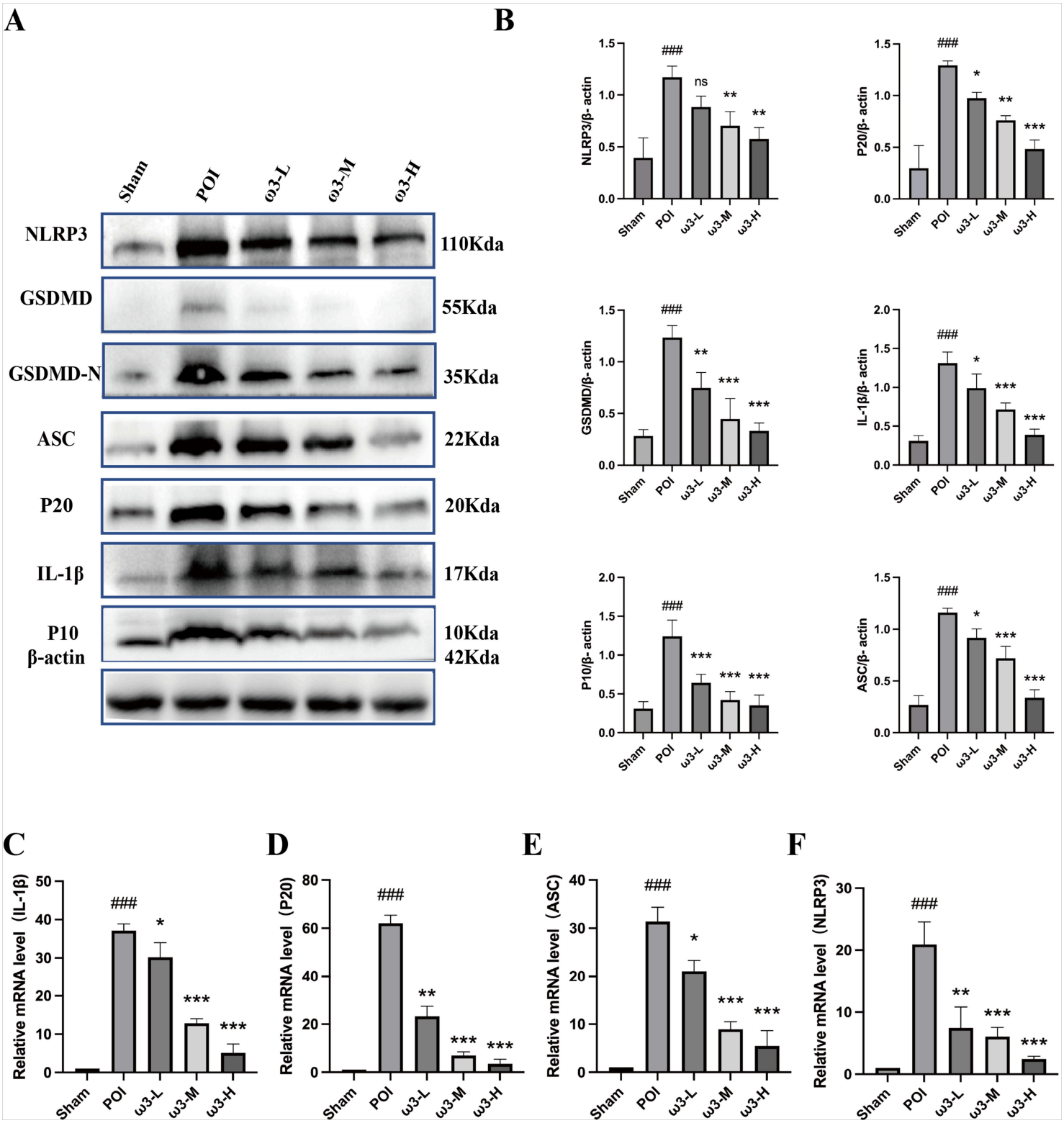


Figure 4

ω-3 PUFAs inhibited activation of the NLRP3/Caspase-1/GSDMD pyroptotic signaling pathway in the ileum of POI mice.(**A**) Representative Western blot bands of NLRP3, GSDMD, GSDMD-N, ASC, Caspase-1 p20, IL-1β, Caspase-1 p10, and β-actin in ileal tissues from the Sham, POI, ω3-L, ω3-M, and ω3-H groups (n = 3). (**B**) Quantitative analysis of NLRP3, Caspase-1 p20, GSDMD, IL-1β, Caspase-1 p10, and ASC protein expression normalized to β-actin (n = 3). (**C–F**) Relative mRNA expression levels of IL-1β, Caspase-1, ASC, and NLRP3 in ileal tissues detected by RT-qPCR (n = 3). Data are presented as the mean ± SD. ###P < 0.001 vs. Sham group; *P < 0.05, **P < 0.01, ***P < 0.001 vs. POI group.

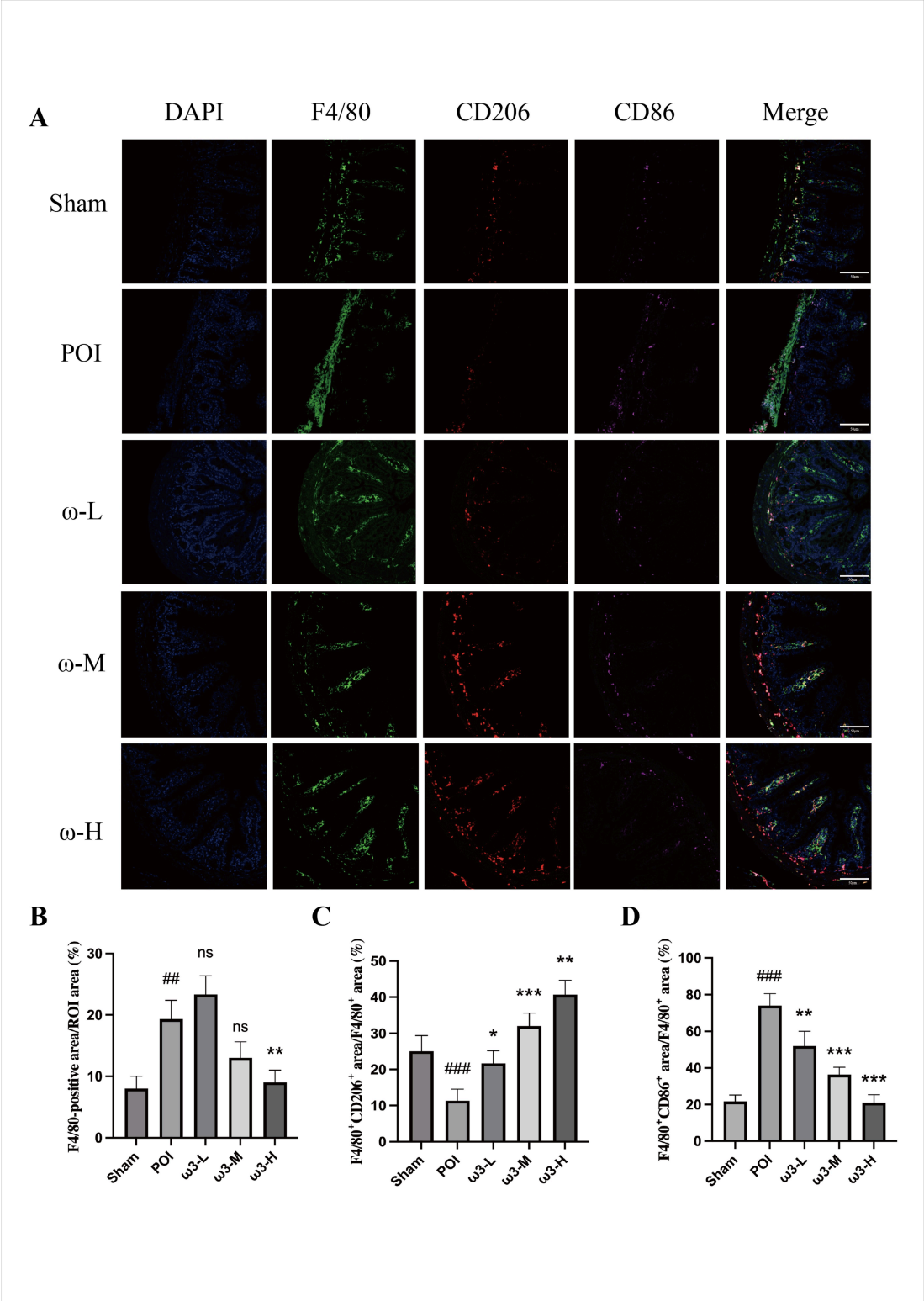


Figure 5

ω-3 PUFAs regulated macrophage infiltration and polarization in the ileum of POI mice. (A) Representative immunofluorescence images of ileal tissues from the Sham, POI, ω3-L, ω3-M, and ω3-H groups. F4/80 (green) was used as a pan-macrophage marker, CD86 (red) as an M1-like macrophage marker, and CD206 (magenta) as an M2-like macrophage marker. Nuclei were counterstained with DAPI (blue). Scale bar = 50 μm. (B) Quantification of the F4/80-positive area relative to the total region of interest (ROI). (C) Quantification of the $F4/80^{+}CD206^{+}$ colocalized area relative to the F4/80-positive area. (D) Quantification of the $F4/80^{+}CD86^{+}$ colocalized area relative to the F4/80-positive area. Data are presented as the mean ± SD (n = 3). ##P < 0.01 and ###P < 0.001 vs. the Sham group; *P < 0.05, **P < 0.01, ***P < 0.001, and ****P < 0.0001 vs. the POI group; ns, not significant. Scale bar = 50 μm.

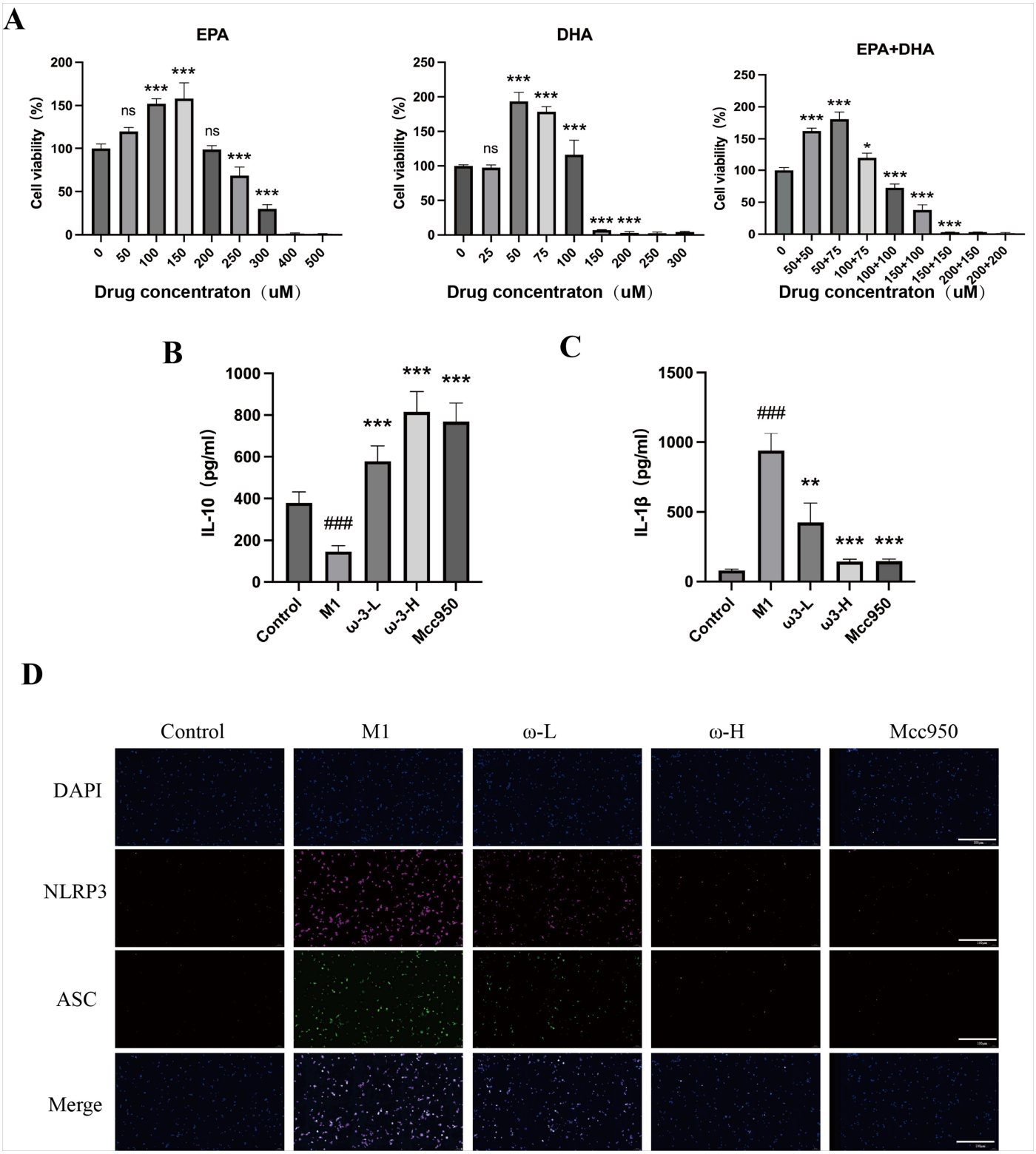


Figure 6

ω-3 PUFAs suppressed inflammatory responses and NLRP3 inflammasome assembly in THP-1-derived macrophages.(**A**) CCK-8 assay showing THP-1 cell viability after treatment with different concentrations of EPA, DHA, or EPA+DHA. (**B and C**) ELISA detection of IL-10 and IL-1β levels in each group, respectively (n = 6). (**D**) Representative immunofluorescence images of NLRP3 and ASC

colocalization. Nuclei were stained with DAPI. Scale bar = 100 μm. Data are presented as the mean ± SD. ###P < 0.001 vs. Control; *P < 0.05, **P < 0.01, ***P < 0.001 vs. M1 group.

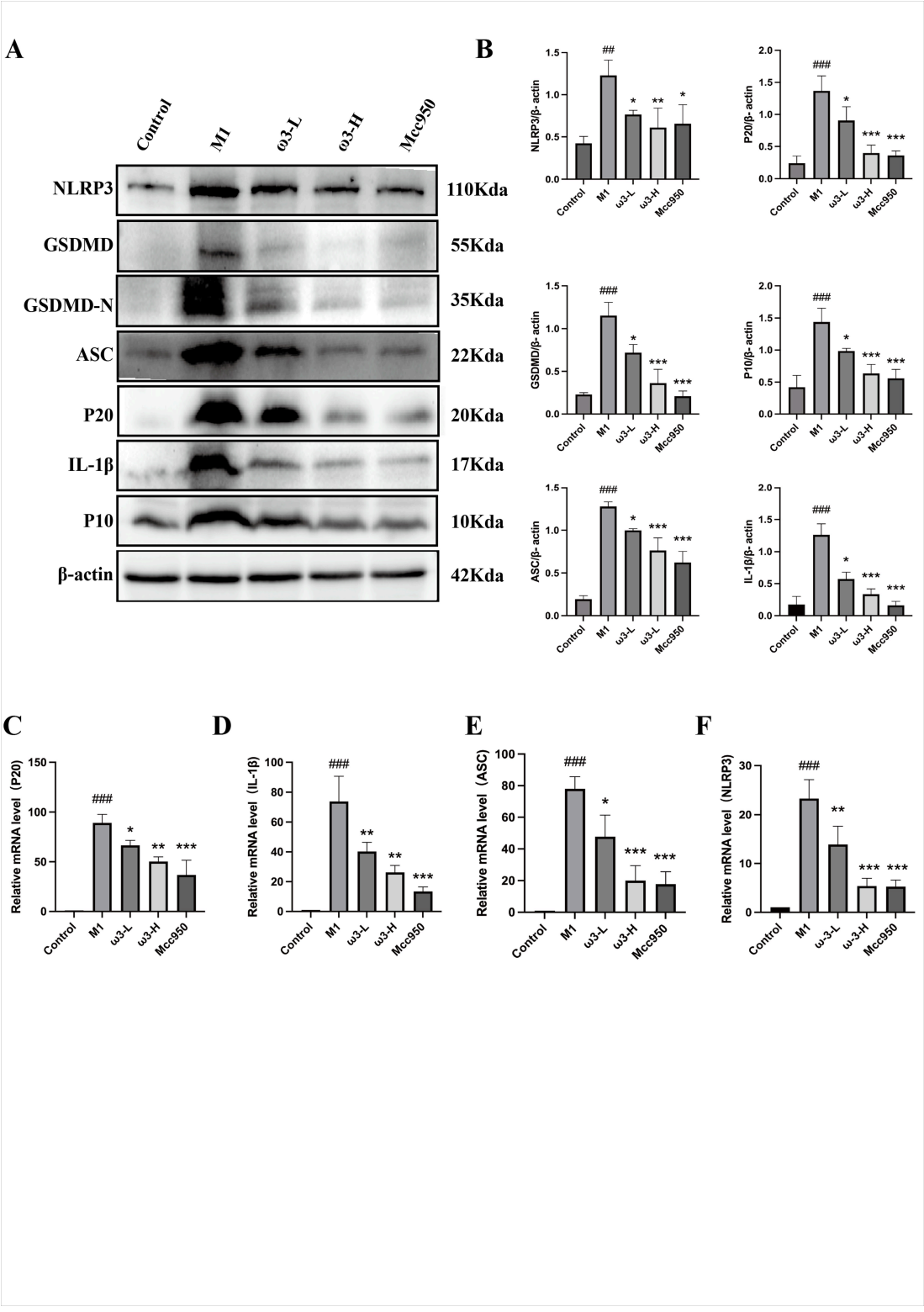


Figure 7

ω-3 PUFAs inhibited NLRP3 inflammasome activation and pyroptosis-related signaling in M1 macrophages.(A) Representative Western blot bands of NLRP3, GSDMD, GSDMD-N, ASC, Caspase-1 p20,

IL-1β, Caspase-1 p10, and β-actin in each group. (B) Quantitative analysis of related protein expression normalized to β-actin. (C–F) Relative mRNA expression levels of Caspase-1, IL-1β, ASC, and NLRP3 detected by RT-qPCR. Data are presented as the mean ± SD (n = 3). ##P < 0.01, ###P < 0.001 vs. Control; *P < 0.05, **P < 0.01, ***P < 0.001 vs. M1 group.

Supplementary Files

This is a list of supplementary files associated with this preprint. Click to download.

- Supplementarymaterial.pdf